Available online at www.sciencedirect.com
SCIENCE DIRECT®
Journal of Nuclear Materials 350 (2006) 195–201
journal of nuclear materials
www.elsevier.com/locate/jnucmat

The effect of alloying modifications on hydrogen uptake of zirconium-alloy welding specimens during corrosion tests

M.Y. Yao [a,*], B.X. Zhou [a], Q. Li [b], W.Q. Liu [b], Y.L. Chu [b]

[a] *Institute of Materials, Shanghai University, Shanghai 200072, PR China*
[b] *The Key Laboratory for Advanced Micro-Analysis, Shanghai University, Shanghai 200444, PR China*

Received 14 July 2004; accepted 27 December 2005

Abstract

The hydrogen uptake behavior during corrosion tests for electron beam welding specimens made out of Zircaloy-4 and zirconium alloys with different compositions was investigated. Results showed that the hydrogen uptake in the specimens after corrosion tests increased with increasing Cr content in the molten zone. This indicated that Cr element significantly affected the hydrogen uptake behavior. Fe and Cr have a low solubility in α-Zr and exist mainly in the form of $Zr(Fe,Cr)_2$ precipitates, which is extremely reactive with hydrogen in its metallic state. It is concluded that the presence of $Zr(Fe,Cr)_2$ second phase particles (SPPs) is responsible for the increase in the amount of hydrogen uptake in the molten zone of the welding samples after corrosion, as $Zr(Fe,Cr)_2$ SPPs embedded in α-Zr matrix and exposed at the metal/oxide interface could act as a preferred path for hydrogen uptake.

1. Introduction

Welding is a necessary process during fabricating fuel rods and fuel assemblies with Zircaloy-4 cladding, and electron beam welding is one of the commonly-used methods [1,2]. Zhou et al. [3] found that after Zircaloy-4 plates were welded to form butt joints by electron beam welding, the corrosion resistance of welding seams was poor. White-oxide films were formed on the surface of the molten zone after autoclave tests at 400 °C in 10.3 MPa H_2O steam for 3–14 days, but the oxide films on the surface of heat affected zone (HAZ) were still black. Kass [1] proposed that the change in microstructure during welding and subsequent fast cooling was the main reason for the reduction in the corrosion resistance. In an effort to simulate the thermal process of electron beam welding, the microstructure and corrosion resistance of Zircaloy-4 after β-quenching or reheating at 700 °C were investigated, which indicated that no white-oxide films on Zircaloy-4 samples were formed after corrosion tests in autoclave at 400 °C in 10.3 MPa H_2O steam for 3–14 days [4].

The loss of the alloying elements such as Sn, Fe, Cr in the molten zone during electron beam welding was the main reason for the poor corrosion resistance of welding seams [2]. Up to 40–50% loss of Sn, Fe, Cr in the molten zone was detected, which brought

* Corresponding author. Tel.: +86 21 5633 7032; fax: +86 21 5633 3870.
E-mail address: yaomeiyi@staff.shu.edu.cn (M.Y. Yao).

0022-3115/$ - see front matter © 2006 Elsevier B.V. All rights reserved.
doi:10.1016/j.jnucmat.2005.12.005

about a deleterious effect on the corrosion resistance after Zircaloy-2 samples joined by vacuum electron beam welding [5]. Our previous work [3] also showed that the degradation of corrosion resistance of zirconium-alloy welding seams was mainly due to the loss of the alloying elements, Sn, Fe and Cr. We employed the zirconium alloy plates, which contained higher amounts of alloying elements than Zircaloy-4, or with further addition of Nb, to make butt joints with Zircaloy-4 plates. The corrosion resistance of welding seams was improved, due to the compensation of the loss of alloying elements in the molten zone or/and the presence of Nb.

Additionally, during corrosion of zirconium alloys at an elevated temperature in pressurized water reactors, the hydrogen uptake occurs to degrade the mechanical properties inevitably. The failure of zirconium alloy parts caused by hydrogen-induced delayed cracking (HIDC) was detected [6,7]. Studies in the past 30 years have indicated that the corrosion resistance, hydrogen uptake and the concomitant HIDC are the main mechanisms for the failure of the zirconium alloys used as nuclear fuel cladding as well as the other parts in reactors [6–9]. So, hydrogen ingress in zirconium alloy is receiving more attention.

In this work, the hydrogen uptake behavior for these welding specimens was studied by examining the amount of zirconium hydrides after corrosion tests. The effect of alloying modifications on hydrogen uptake of zirconium alloys was then discussed.

2. Experimental procedure

2.1. Welding samples preparation

The alloying compositions of zirconium-alloy strips with 2 mm (W) × 1.5 mm (T) are listed in Table 1. Two strips with the same composition (such as #1) were welded alternately with three strips of #4 (Zircaloy-4) into butt joints by means of vacuum electron beam welding, as shown schematically in Fig. 1, which also shows the positions of composition analysis. The thermal history of the welding seams was complicated and different at different locations as four welding seams were welded sequentially. The completed welding seams were reheated into β- or α-phase region during the welding of the next seams. For simplification, the samples where #1 strips were welding alternately with #4 strips were denoted as 1-4 welding samples. The rest may be denoted by analogy as 2-4, 3-4 and 4-4 welding samples.

Table 1
The composition of zirconium alloys (in mass fraction %)

Strip numbers	Alloy elements				
	Sn	Fe	Cr	Nb	Zr
#1 (1.97Sn–0.37Fe–0.23Cr–Zr)	1.97	0.37	0.23	/	Bal
#2 (1.92Sn–0.32Fe–Zr)	1.92	0.32	/	/	Bal
#3 (1.88Sn–0.35Fe–0.52Nb–Zr)	1.88	0.35	/	0.52	Bal
#4 (Zircaloy-4)	1.50	0.20	0.10	/	Bal

2.2. Composition analysis

The compositions in different positions at 50 μm from the welding surface, were analyzed by an electron microprobe. The relative contents of Sn, Fe and Cr in each position were obtained by comparing their peak intensities with those in Zircaloy-4, respectively; the relative content of Nb in different positions was obtained in the same way by comparing the peak intensity of Nb with that in #3 strips. Note that the ZAF corrections were not performed due to the slight difference of alloying elements in absolute amount between the different positions and Zircaloy-4, as well as the lower content of Sn, Fe and Cr in different positions on the welding surface and in Zircaloy-4.

2.3. Corrosion tests

Welding specimens with four welding seams, were cut in 10 mm length perpendicularly to welding seams by spark cutting (see Fig. 1 for the cutting location). On the welding surface, the area of molten zone occupied more than 80%; on the reverse side of welding surface, the area of molten zone occupied less than 20%; the rest of un-molten area was composed of about 60% of Zircaloy-4 and about 40% of modified zirconium alloys. These samples were divided into two groups, each one having three specimens. One group annealed at 500 °C for 1.5 h to relieve the welding stress is marked X-A, the other without annealing is marked X-NA, where X corresponds to the name of welding sample denoted in Section 2.1, such as 1-4. The corrosion tests of the welding specimens were carried out in autoclave at 400 °C in 10.3 MPa H_2O steam for 165 days. Prior to the corrosion tests, the specimens were cleaned and pickled in a solution of 10% HF + 45%HNO_3 + 45%H_2O (in volume), and then rinsed in cold tap water and boiling deionized water.

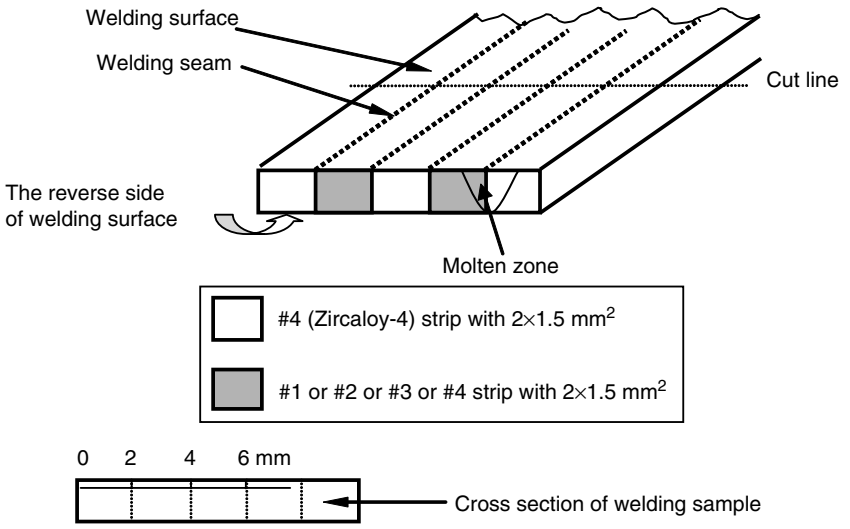

Fig. 1. Schematic diagram of a welding sample.

2.4. Examination of hydrides and SPPs

Some sections of the corroded specimens were prepared by grinding, polishing and etching in a solution of $10\%HF + 10\%H_2O_2 + 80\%HNO_3$ (in volume) to reveal the hydrides. Optical microscopy was employed to examine the morphology and distribution of the hydrides. SPPs in the welding specimens were examined by a JSM-6700 F scanning electron microscope (SEM) after pickling in a solution of $10\%\ HF + 45\%HNO_3 + 45\%H_2O$ (in volume).

3. Experimental results

3.1. The relative content of Sn, Fe, Cr and Nb on the section of welding sample

Fig. 2 illustrates the variation of alloying elements in the molten zone of 4-4 and 3-4 welding samples. It was shown that the composition of the molten zone, which was a mixture of two welded alloys, was different from that of HAZ. In 4-4 welding sample, the compositions in the two welded strips were same before welding, but the composition of molten zone was still different from that of HAZ due to the evaporation of alloying elements during welding.

For 4-4 welding specimen (Fig. 2(a)), Sn, Fe and Cr contents in the molten zone were about 60%, 50% and 30% of those in Zircaloy-4, respectively, while after adding higher amounts of alloying additions to compensation for their evaporation, the alloying contents were similar to those in Zircaloy-4. For example, in 3-4 welding specimen (Fig. 2(b)), Sn and Fe contents in the molten zone were nearly the same as those in Zircaloy-4. It was found that Cr content in the molten zone of 3-4 welding specimen was much lower due to no Cr in #3 strips.

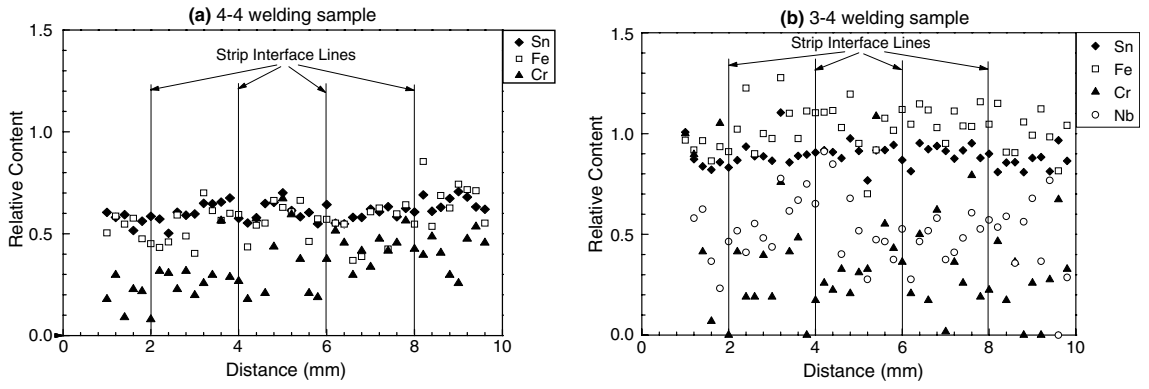

Fig. 2. The relative content of Sn, Fe, Cr and Nb on the section of welding samples.

In addition, the evaporation of Nb during welding is minimal because of its low evaporation pressure. Therefore, the relative content of Nb in the molten zone was about 40–60% of that in #3 strip, which was equal to an average content of #3 and #4 strips mixed in the molten zone.

For 2-4 welding specimen, similar to 3-4 welding specimen, the contents of Sn and Fe in the molten zone were also compensated, and the content of Cr in the molten zone was also much lower due to no Cr in 2# strips. For 1-4 welding specimen, the contents of Sn, Fe and Cr in the molten zone were all compensated.

3.2. The morphology and distribution of zirconium hydrides in the molten zone

Fig. 3 shows the morphology and distribution of zirconium hydrides in the molten zone of the corroded specimens. In order to relate hydrogen uptake with the weight gain, the data of the weight gains [3] is listed in Table 2. It was found that the hydrogen uptake in the molten zone after corrosion tests was out of proportion to the weight gain. The amount of zirconium hydrides in 1-4-A was comparative to that in 4-4-A, although the weight gain of 1-4-A was 20 times lower than that of 4-4-A. The amount

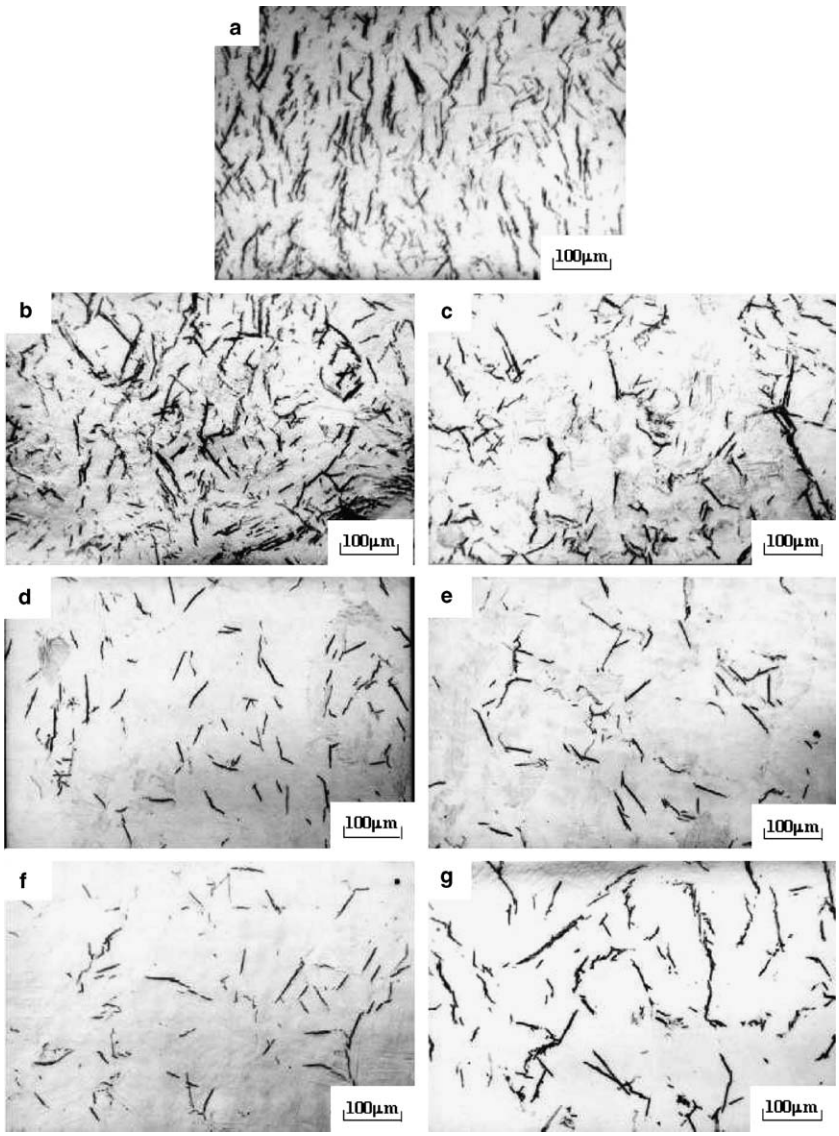

Fig. 3. Optical micrographs of zirconium hydrides in molten zone of welding specimens: (a) 4-4-A, (b) 1-4-A, (c) 1-4-NA, (d) 2-4-A, (e) 2-4-NA, (f) 3-4-A and (g) 3-4-NA.

Table 2
The weight gain of welding specimens tested in autoclave at 400 °C, 10.3 MPa H_2O steam for 165 days [3]

Samples	Weight gain (mg/dm^2)
4-4-A	2470
1-4-A[a]	122.5
1-4-NA[b]	123.9
2-4-A	207.6
2-4-NA	251.4
3-4-A	86.2
3-4-NA	352.7

[a] The samples were annealed at 500 °C for 1.5 h.
[b] The samples were not annealed.

of zirconium hydrides in 1-4-A and 1-4-NA was noticeably larger than that in 2-4-A, 2-4-NA and 3-4-NA, while the weight gains of the former two specimens were less than those of the latter three ones. Note that #1 strips contained higher Cr content than #4 ones, while #2 and #3 strips did not contain Cr, which resulted in the decrease of Cr content in the molten zone in the sequence of 1-4, 4-4 and 2-4/3-4 welding samples [3]. This indicates that Cr content in the molten zone of welding specimens significantly affects the hydrogen uptake behavior.

Additionally, annealing had a more or less effect on hydrogen uptake of welding samples. For 1-4 welding samples, the amount of zirconium hydrides in 1-4-A was more than that in 1-4-NA, while their weight gains were comparative. For 2-4 welding samples, the amount of zirconium hydrides in 2-4-A was a little more than that in 2-4-NA, although the weight gain of 2-4-A was a little lower than that of 2-4-NA. For 3-4 welding sample, the amount of zirconium hydrides in 3-4-A was a little less than that in 3-4-NA, however, the weight gain of 3-4-A was much lower than that of 3-4-NA.

3.3. The morphology and distribution of SPPs in the molten zone

Fig. 4 shows the morphology and distribution of SPPs in the molten zone of 1-4-A, 1-4-NA, 2-4-A and 2-4-NA. The amount of SPPs in the specimens increased after annealing at 500 °C. It is easy to understand that since the specimens were rapidly cooled from high temperature during welding, Fe and Cr could be supersaturated in α-Zr solid solution; after being annealed at 500 °C for 1.5 h, part of the alloying elements supersaturated in α-Zr could precipitate as SPPs. In other way, it was reported that the Fe/Cr rario in $Zr(Fe,Cr)_2$ SPPs was 2.1–2.5 after Zircaloy-4 specimen cooling from β phase, and reduced to 1.5–1.9 after annealing in α-phase [10], so the Fe/Cr ratio in $Zr(Fe,Cr)_2$ SPPs maybe decrease after annealing at 500 °C. In view of

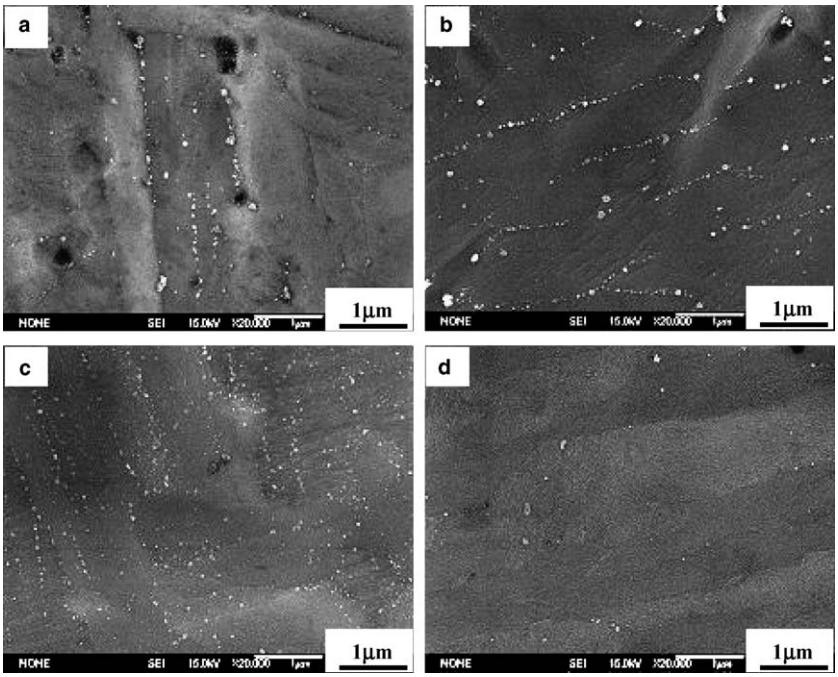

Fig. 4. SEM micrographs of the SPPs in different welding specimens: (a) 1-4-A, (b) 1-4-NA, (c) 2-4-A and (d) 2-4-NA.

alloying compositions in the molten zone [3], most of SPPs in 1-4-A and 1-4-NA were $Zr(Fe,Cr)_2$ for higher Cr content , but most of them in 2-4-A were $ZrFe_2$ for much lower Cr content.

4. Discussion

4.1. The effect of Cr element on the hydrogen uptake

It has been reported that the SPPs in Zircaloy play an important role on hydrogen uptake behavior during corrosion tests [9,11]. Fe, Cr and Ni have low solubility in α-Zr and exist mainly in the form of $Zr(Fe,Cr)_2$ and $Zr_2(Fe,Ni)$ SPPs for Zircaloy-2 and $Zr(Fe,Cr)_2$ SPPs for Zircaloy-4 [12–14]. Thus, it is proposed that the effect of Cr element on the hydrogen uptake behavior of zirconium alloys is closely related to the formation of $Zr(Fe,Cr)_2$ SPPs.

Prior studies reveal that $Zr(Fe,Cr)_2$ intermetallic phase is extremely reactive with hydrogen in its metallic state and its hydrogen absorption is faster than that of Zr. Moreover, the amount of hydrogen absorption of $Zr(Fe,Cr)_2$ intermetallic compound increases with increasing Cr content, i.e., with decreasing the ratio of Fe/Cr [15] (see Table 3). It is known that ZIRLO and E635 zirconium alloys without Cr, have lower hydrogen uptake than Zircaloy-4. For example, Zhou et al. [16] reported that a zirconium alloy with a composition similar to ZIRLO had only 30% hydrogen content compared with the same-size Zircaloy-4 specimens after corrosion in 400 °C H_2O steam at the same level of 100 mg/dm^2 weight gain. It is suggested that the increase of hydrogen uptake in zirconium alloys with Cr should be closely related to the presence of $Zr(Fe,Cr)_2$ SPPs.

In view of the very low diffusion coefficients of hydrogen in zirconia, as measured by Khatamian [17] and estimated by Cox and Roy [18], the performance of hydrogen uptake can not itself explain the level of hydrogen absorption generally found in zirconium alloys, which is systematically higher than that predicted by calculations of hydrogen diffusion in zirconia. Transmission electron microscopy (TEM) observations of oxide films on Zircaloy-4 showed that oxidation rate of $Zr(Fe,Cr)_2$ precipitates was slower than that of the zirconium matrix [19]. Tägtstrom et al. [9] and Leliëvre et al. [20] proposed that SPPs offered sites where hydrogen could easily be absorbed into the Zr-based material. Therefore, it's reasonable to propose that the presence of $Zr(Fe,Cr)_2$ SPPs is responsible for the increase in the amount of hydrogen uptake, as $Zr(Fe,Cr)_2$ SPPs embedded in α-Zr matrix and exposed at the metal/oxide interface could act as a preferred path for hydrogen uptake. This can be used to explain why the hydrogen uptake in the molten zone of the welding specimens after corrosion tests is out of proportion to the weight gain.

Table 3
Hydrogen storage data of $Zr(Fe_xCr_{1-x})_2$ intermetallic compounds [15]

Compounds	$ZrCr_2$	$Zr(Fe_{0.5}Cr_{0.5})_2$	$Zr(Fe_{0.75}Cr_{0.25})_2$	$ZrFe_2$
Hydrogen capacity (H/M)	1.3	1.13	0.95	0.05

H/M: hydrogen to metal ratio, in moles.

4.2. The effect of annealing on the hydrogen uptake

Annealing had a more significant effect on hydrogen uptake in 1-4 welding specimen, while it had a slight effect on hydrogen uptake in 2-4 one. Based upon the above discussion and the examination of SPPs, the effect of annealing on hydrogen uptake is mainly due to the change in amount, size and distribution of $Zr(Fe,Cr)_2$ SPPs, as well as Fe/Cr ratio in $Zr(Fe,Cr)_2$ SPPs.

Annealing also had an effect on hydrogen uptake in 3-4 welding specimen. The percent of theoretical hydrogen pickup for 3-4-A was higher than for 3-4-NA. This can be explained by the difference in corrosion resistance which was more significant on the reverse side of the welding surface. The oxide films on the surface of #3 strips, which were located on the reverse side of welding surface, were much thicker in 3-4-NA (80 μm) than in 3-4-A (3-4 μm) [21]. It was reported [22] that the presence of β-Zr in Zr–Nb alloys reduced the corrosion resistance, and the decomposition of β-Zr into α-Zr and β-Nb could improve it. TEM observation also showed that β-Zr, which resulted from higher Nb content in #3 strips on the reverse side of welding surface, was decomposed to form α-Zr and β-Nb after annealing at 500 °C [21].

5. Conclusion

(1) The higher Cr content in the molten zone of the welding samples resulted in higher hydrogen uptake. The hydrogen uptake was out of

proportion to the weight gain after corrosion tests. This can be attributed to the hydrogen absorption of $Zr(Fe,Cr)_2$ SPPs in the specimens, as the $Zr(Fe,Cr)_2$ SPPs embedded in α-Zr matrix and exposed at the metal/oxide interface could act as a preferred path for hydrogen uptake.

(2) While adding a small amount of Nb into the Cr-free zirconium alloys was helpful to improve the corrosion resistance, it had only a small effect on the hydrogen uptake behavior.

Acknowledgements

This project is financially supported by the National Nature Science Foundation of China (50371052) and Shanghai Leading Academic Discipline Project (T0101).

References

[1] S. Kass, WAPD-TM-972, 1973.
[2] S.G. McDonald et al., Zirconium in the Nuclear Industry: Fifth International Conference ASTM STP 754, 1982, pp. 412.
[3] B.X. Zhou, Q. Li, Z. Miao, et al., Nucl. Power Eng. 24 (3) (2003) 236 (in Chinese).
[4] B.X. Zhou, Q. Li, Z. Miao, J. Nucl. Power Eng. 21 (2000) 339 (in Chinese).
[5] B.X. Zhou, S.K. Zheng, S.X. Wang, Chinese J. Nucl. Sci. Eng. 8 (2) (1988) 130.
[6] E.C.W. Perryman, Nucl. Energy. 17 (1978) 95.
[7] C.J. Simpson, C.E. Ells, J. Nucl. Mater. 52 (1974) 289.
[8] R.A. Ploc, Zirconium in the Nuclear Industry: Thirteenth International Symposium, ASTM STP 1423, 2002, p. 297.
[9] P. Tägstrom, M. Limbäck, M. Dahlbäck, T. Andersson, H. Pettersson, Zirconium in the Nuclear Industry: Thirteenth International Symposium, ASTM STP 1423, 2002, p. 96.
[10] B.X. Zhou, X.L.Yang, China Nuclear Science and Technology Report, CNIC-01074, SINER-0066, 1996.
[11] P. Barberis, E. Ahlberg, et al., Zirconium in the Nuclear Industry: Thirteenth International Symposium, ASTM STP 1423, 2002, p. 33.
[12] M. Harada, M. Kimpara, A. Kastuhio, Zirconium in the Nuclear Industry: Ninth International Symposium, ASTM STP1132, 1991, p. 368.
[13] J.S. Forster, R.L. Trapping, T.K. Alexander, D. Philips, T. Laursen, J.R. Leslie, Nucl. Instr. Meth. B 64 (1992) 403.
[14] S. Kass, W.W. Kirk, ASM Trans. Quart. 56 (1962) 77.
[15] D. Shaltiel, I. Jacob, J. Davidov, J. Less-Common Met. 53 (1977) 117.
[16] B.X. Zhou, W.J. Zhao, Z. Miao, et al., Study of New Zirconium Alloys, in: B.X. Zhou, Y.K. Shi (Eds.), Biomaterials and Ecomaterials III-2, Proceedings of 1996 Chinese Materials Symposium, 17–21 Nov. 1996, Chinese Materials Research Society, Chemical Industry Press, Beijing, China, 1997, p. 183 (in Chinese).
[17] D. Khatamian, Z. Phys. Chem. 181 (1993) 435.
[18] B.Cox, C. Roy, AECL Report 2519, 1965.
[19] D. Pêcheur, F. Lefebvre, A.T. Motta, C. Lemaignan, D. Charquet, Zirconium in the Nuclear Industry: Tenth International Symposium, ASTM STP 1245, 1994, p. 687.
[20] G. Leliëvre, C. Tessier, et al, J. Alloy Compd. 268 (1998) 308.
[21] M.Y. Yao, Q. Li, B.X. Zhou, et al., Nucl. Power Eng. 25 (2) (2004) 147 (in Chinese).
[22] K.N. Choo, Y.H. Kang, S.I. Pyun, V.F. Urbanic, J. Nucl. Mater. 209 (1994) 226.